Proceedings of the Combustion Institute, Volume 29, 2002/pp. 329–336

TEMPERATURE REGIONS OF OPTIMAL CHEMICAL INHIBITION OF PREMIXED FLAMES

M. D. RUMMINGER,* V. I. BABUSHOK AND G. T. LINTERIS
National Institute of Standards and Technology
Gaithersburg, MD 20899-8665, USA

Chemically active fire suppressants may, due to their properties or the means by which they are added to flames, have strong inhibition effects in particular locations in a flame. To study the spatial effects of chemically active inhibitors, numerical experiments are conducted in which the rates of reactions of model inhibitors are varied in spatial regions defined by temperature. The influence of three types of spatial regions are investigated, those with the inhibitor (1) active only within a narrow temperature band (off-on-off), (2) active below a cutoff temperature (on-off), and (3) active above a cutoff temperature (off-on). The effect of several localized chemical perturbations on the burning velocity are studied, including the variation of the $H + O_2 \leftrightarrow OH + O$ or the $CO + OH \leftrightarrow CO_2 + H$ reaction rate and catalytic scavenging of radicals by an idealized perfect inhibitor or by CF_3Br (halon 1301). The results indicate that the flame speed is reduced most when the perturbation location corresponds to the regions of maximum radical volume fraction or maximum chain-branching reaction rates. Each of the chemical perturbations has a negligible effect below 1200 K. Calculations for CF_3Br-inhibited flames indicate a temperature of maximum influence that is higher than previous suggestions for Br-based inhibitors. Calculations for flames with the $H + O_2$ rate perturbed or with addition of the perfect inhibitor indicate that the important region for flame inhibition in lean, rich, and stoichiometric flames corresponds to the position of the peak H-atom volume fraction. The results of this work demonstrate that the burning velocity is sensitive to inhibition over a relatively small spatial region of the flame. Simulations with stepwise activation and deactivation of an inhibitor show that the effect of the inhibitor is small when the activation or deactivation temperature is below 1700 K.

Introduction

To facilitate analysis, premixed flames are commonly divided into various zones or regions [1–4]. Understanding the effect of reactions proceeding in different zones of a premixed flame can provide insight into flame structure relevant to flame inhibition. Analysis of the flame zone most sensitive to chemical or thermal inhibition has been an active area of flame inhibition research for many years [5–16]. For example, many researchers have claimed that the important region of action of halogenated agents is the low-temperature region of the flame [6–8, 11, 15–17].

In addition to providing insight into the mechanism of existing flame inhibitors, numerical simulations of flames using complex kinetics and *model* inhibitors allow simulations of inhibitors which have not yet been discovered or synthesized and can provide information useful in the search for new approaches to fire suppression. To study the spatial effects, we perturb the reaction rates of selected chemical reactions in a region that can be defined by temperature, species concentration, time, or space. For example, by varying the region in which inhibition occurs, we can simulate an inhibitor that is effective in a certain temperature range (e.g., inhibiting molecules formed from a precursor which is stable only below a certain temperature). Such simulations can aid in the search for new fire suppressants by allowing researchers to ask exploratory questions about new compounds, even with limited information about the kinetics.

In this paper, we use this technique to investigate flame inhibition, with inhibitor concentrations less than those typically used to suppress fires. Although we do not directly address fire suppression, the magnitude of the burning velocity reduction used here is adequate for demonstrating the technique and gaining insight into flame behavior under these conditions. To this end, we examine numerically the response of premixed flames to several types of perturbation. The effect of the perturbation on the overall reaction rate is assessed through evaluating changes in laminar flame speed. We analyze the effects of perturbations of two shapes: impulsive and stepwise. As the source of the perturbation, we use (1) addition of CF_3Br (halon 1301), (2) addition of a perfect inhibitor, (3) variation of the rate of chain

* Current address: Cleaire Advanced Emission Controls, 14775 Wicks Blvd., San Leandro, CA 94577-6779, USA.

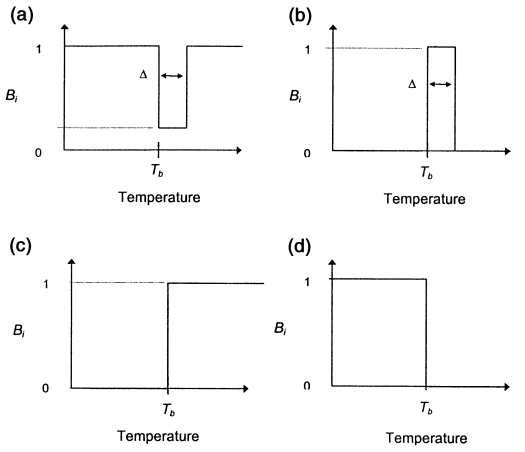

FIG. 1. Shapes of the reaction rate profile B_i used to describe (a) perturbation of chain-branching and heat-release rates, (b) addition of perfect inhibitor and CF_3Br, (c) rapid inhibitor activation, and (d) rapid inhibitor deactivation.

branching, and (4) variation of the heat release rate from CO oxidation.

Numerical Technique

A reacting system is perturbed by modifying selected reaction rates in a region or regions (also called "bands"). The band can be defined by a range of temperature, time, space, or species concentration. The perturbation can affect a single reaction (for example, $H + O_2 \leftrightarrow OH + O$), a class of reactions (for example, CO_2 formation reactions), or a portion of a chemical mechanism (for example, reactions involving Br-containing species in a mechanism for CF_3Br inhibition). In this way, we use model inhibitors to simulate physical behaviors (such as agent phase change) which may limit the chemical action of inhibitor to certain regions of the flame.

For bands defined by temperature, a perturbation factor B_i is defined for the selected group of reactions as

$$B_i = 1, \qquad T < T_b$$

$$0 < B_i < 1, \qquad T_b \le T \le T_b + \Delta$$

$$B_i = 1, \qquad T > T_b + \Delta$$

where T is the gas temperature, T_b is the temperature at the low edge of the band, and Δ is the size of the band. Fig. 1a illustrates the band shape for this example. The reaction rates of the selected reactions are multiplied by B_i, and the rest of the reactions are not directly disturbed (i.e., $B_i = 1$). To study different types of perturbation, the band depth (the magnitude of B_i), width (Δ), and shape (the variation of B_i with T) can be varied. For study of flame inhibition, the pertinent reactions are turned off outside the band ($B_i = 0$) and turned on inside the band ($B_i = 1$), as illustrated in Fig. 1b. For modeling of activation or deactivation of an inhibitor a forward-facing or backward-facing step function is used; here, the inhibition reactions are turned off (or on) below a certain temperature and turned on (or off) above that temperature, as shown in Fig. 1c and d.

In practice, the band is smoothed at the edges to avoid numerical convergence problems caused by infinite gradients. For the computations described here, the smoothing function is $B_i = a - b\,\mathrm{erf}(-cT^* + d)$, where $T^* = (T - T_b)/\Delta$ at the low temperature edge and $T^* = (T_b + \Delta - T)/\Delta$ at the high temperature edge. The constants a, b, c, and d are selected such that the width of the smoothed portion of the band is approximately 0.1Δ at each end.

Flame Modeling Approach

The Sandia flame code PREMIX [18], with the kinetic [19] and transport [20] subroutines, is used to simulate the freely propagating premixed flame. (*Note:* Certain commercial equipment, instruments, or materials are identified in this paper to adequately specify the procedure. Such identification does not imply recommendation or endorsement by the National Institute of Standards and Technology, nor does it imply that the materials or equipment are necessarily the best available for the intended use.) The CHEMKIN subroutine CKRAT is modified to accommodate the chemical behavior of the model inhibitors. Part of the postprocessing is performed using a graphical postprocessor [21]. For all calculations, the initial reactant temperature is 300 K and the pressure is 0.10133 MPa. The "GRAD" parameter is set to 0.15, and "CURV" is set to 0.35 for all of the calculations, except those involving CF_3Br, where higher values of GRAD (0.35) and CURV (0.55) are used to reduce the calculation time. The former values of GRAD and CURV yield 90–125 active grid points in the calculation, and the latter, 65 grid points. As discussed in Ref. [22], the calculated burning velocity is estimated to be reduced about 6% for an infinite number of grid points. In order to keep the large number of calculations in the present work tractable, we accept this small error, which is believed to be unimportant for the investigations presented here.

The kinetic and thermodynamic data of GRI-MECH 1.2 [23] (32 species and 177 chemical reactions) serve as a basis for describing the methane combustion, except when the inhibitor is CF_3Br. In that case, the mechanism of Babushok et al. [24] describes the C_1/C_2 hydrocarbon chemistry and the halogen chemistry (70 species and 595 reactions)

TABLE 1
Input parameters and calculated temperatures and flame speed for the flames simulated in this paper

Perturbation	ϕ	B_i Inside Band	B_i Outside Band	Inhibitor Volume Fraction	T_{max} (K)	$S_{L,0}$[a] (cm/s)	$S_{L,all}$[b] (cm/s)	$S_{L,min}$[c] (cm/s)	T_c for $S_{L,min}$ (K)
$H + O_2$	0.7	0.45	1.0	n.a.	1850	20.7	n.c.	15.5	1550
$H + O_2$	1.0	0.45	1.0	n.a.	2235	41.2	n.c.	31.0	1800
$H + O_2$	1.3	0.45	1.0	n.a.	2056	25.2	n.c.	18.0	1850
CO + OH	1.0	0.1	1.0	n.a.	2235	41.2	n.c.	29.1	1850
Perfect	0.7	1.0	0.0	2.0×10^{-5}	1850	20.7	13.8	16.2	1650
Perfect	1.0	1.0	0.0	4.0×10^{-5}	2235	41.2	27	30.9	1950
Perfect	1.3	1.0	0.0	2.6×10^{-5}	2056	25.2	16.8	18.3	2000
CF_3Br	1.0	1.0	10^{-4}	0.00755	2235	41.2[d]	26.4	29.2	1750

Note: n.a. = not applicable; n.c. = not calculated. For $H + O_2$ and CO + OH, the smoothing function constants are $a = 0.55$, $b = 0.45$, $c = 60$, $d = 57$. For the perfect inhibitor, the smoothing function constants are $a = 0.5$, $b = 0.5$, $c = 60$, $d = 57$.

[a] Flame speed of the unperturbed or uninhibited flame.

[b] Flame speed with perturbation throughout flame.

[c] Minimum flame speed with perturbation in a bandwith of 300 K.

[d] The flame speed is 39.0 cm/s when the halogen chemistry is turned off throughout the flame because of the physical effects of CF_3Br.

(note that Ref. [24] also provides experimental verification of the CF_3Br mechanism).

The perfect inhibitor model [25] represents an upper limit to the catalytic action of an inhibitor. The model assumes that the inhibitor-containing species In and InX (in which X is a flame radical H, O, or OH), react with radicals at gas-kinetic rates. For example, $In + H \Rightarrow InH$, followed by $InH + OH \Rightarrow In + H_2O$. All reactions are bimolecular, with an activation energy and temperature exponent of 0 and a pre-exponential factor of 1×10^{14} $cm^3 \cdot s \cdot mol^{-1}$; the transport properties of Ar are used for the species In and InX. The perfect inhibitor species are present at low concentrations, so their contribution to the energy balance is small; also, since the reactions for these species are listed as forward rates, the choice of thermodynamic properties for these species does not affect their reaction rates. The perfect inhibitor reactions [25] are combined with those of GRI-MECH 1.2. Since the perfect inhibitor mechanism is a theoretical construct, it can not be experimentally verified. Nonetheless, it has been compared with the experimental results for inhibition by the very powerful flame inhibitor $Fe(CO)_5$ and found to give burning velocity reductions reasonably close to that agent [25].

A stoichiometric, freely propagating premixed CH_4/air flame is perturbed in temperature bands of $\Delta = 300$ K. The following four types of perturbation are used:

1. Reduction of the rate of chain branching by $H + O_2 \leftrightarrow OH + O$ (referred to as "$H + O_2$" below), because it provides a majority of the chain branching at high temperature
2. Reduction of the rate of heat release by $CO + OH \leftrightarrow CO_2 + H$ (referred to as "CO + OH" below), because of its importance in determination of the final flame temperature
3. Catalytic scavenging of radicals (O, OH, and H) by a perfect inhibitor [25], to investigate the maximum inhibition effect
4. Inhibition by CF_3Br, because it is used as a benchmark in flame inhibition studies

The band width of 300 K was selected after conducting extensive numerical experiments with different band widths ranging from 50 to 2000 K. The results consistently showed that the location of maximum inhibition was independent of the width of the band. The minimum burning velocity decreased as the band became wider, but the band-center temperature of minimum burning velocity remained nearly constant for the perturbation considered. The choice of a 300 K bandwidth was made as a compromise between having too little effect (a 100 K band only decreased burning velocity by 15%) and being too wide to provide insight into the inhibition mechanisms.

Selected input parameters and calculated results for the flames simulated in this paper are listed in Table 1. For the $H + O_2$ and CO + OH perturbation, the reaction of interest is unaffected outside the band ($B_i = 1$) and damped inside the band ($B_i = 0.45$ for $H + O_2$, $B_i = 0.1$ for CO + OH). Thus, the reduction in heat release for the CO + OH reaction is achieved through a reduction in the rate of this reaction within the band. For the perfect inhibitor, reactions involving the perfect inhibitor are turned off outside the band ($B_i = 0$) and turned

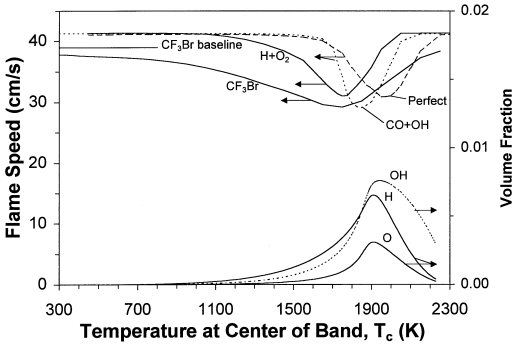

FIG. 2. Variation of flame speed (left axis) for four types of perturbation: reduction of the H + O_2 ↔ OH + O or CO + OH ↔ CO_2 + H reaction rate and inhibition by a perfect agent or CF_3Br. The "CF_3Br baseline" refers to the flame speed when the halogen chemistry is damped by 10^{-4}. The bandwidth Δ is 300 K, so the band extends 150 K below and above the temperature shown on the x-axis. The calculated volume fraction of OH, H, and O (right axis) is shown for an uninhibited stoichiometric methane/air flame.

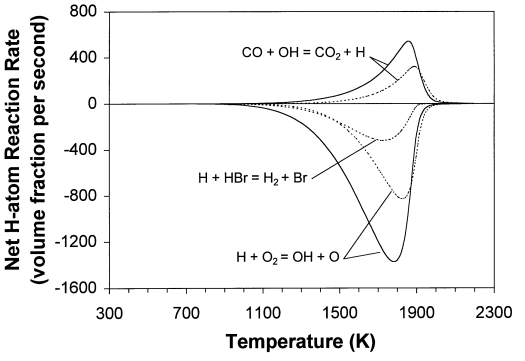

FIG. 3. Net H-atom reaction rate for three important reactions in stoichiometric methane/air flames. Solid lines: uninhibited flame; dashed lines: CF_3Br-inhibited flame (agent volume fraction of 0.00755).

on inside the band ($B_i = 1$). The volume fraction of the perfect inhibitor in the unburned gas is 4.0×10^{-5}, which results in a flame speed (S_L) of 27 cm/s when the inhibitor is active throughout the flame (note that $S_L = 41$ cm/s for the uninhibited flame).

For inhibition by CF_3Br, the reactant stream consists of a stoichiometric mixture of methane and air and a volume fraction of added CF_3Br of 0.0755, resulting in a one-third reduction in flame speed (to 26.4 cm/s) when the inhibitor is active throughout the flame. While the amount of inhibitor which produces a one-third reduction of flame speed is less than that typically used to suppress fires, this perturbation to the flame is adequate for demonstrating the region of greatest influence. Ideally, when simulating the model inhibitors, the reactions involving Br- and F-containing species would be turned on ($B_i = 1$) in the band and turned off outside the band ($B_i = 0$). Because of convergence problems compounded by the size of the mechanism, we use $B_i = 10^{-4}$ for the halogen chemistry outside the band.

Results and Discussion

Figure 2 shows the response of the flame to each of the perturbations. (Note that the kinks in some of the curves of Fig. 2, as well as Fig. 4 and Fig. 6, are caused by a somewhat coarse progression of calculated band-center temperatures and are not present if a finer series of calculations are made.) The reduction in flame speed for H + O_2 and CO + OH can only be compared qualitatively to results for the perfect inhibitor and CF_3Br, because of the different value of B_i in the bands. The minimum flame speed occurs at a band-center temperature (T_c) of 1750 K for CF_3Br, 1800 K for H + O_2, 1850 K for CO + OH, and 1950 K for the perfect inhibitor. Using reaction flux analyses, it is possible to infer that perturbations at these temperatures would most strongly affect the burning velocity of the flames. For H + O_2 and CO + OH, these temperatures correspond to the maximum reaction rate of the affected reaction (as shown in Fig. 3). Similarly, for the perfect inhibitor, the temperature is near the temperature corresponding to the peak volume fractions of O, H, and OH (as shown in Fig. 2).

The difference in location of peak effectiveness of CF_3Br versus the perfect inhibitor is caused by the shift of the partial equilibrium of the scavenging reactions. For CF_3Br at higher temperature, the equilibrium for the inhibition reaction H + HBr ↔ H_2 + Br shifts to the left [9], reducing the effectiveness.

In earlier studies of inhibition of premixed flames by CH_3Br, CF_3Br, and HBr, it was argued that the primary inhibition occurs upstream of the main reaction zone. Wilson [7] and Wilson et al. [8] investigated inhibition of low-pressure (5.1 kPa) methane/oxygen flames inhibited by CH_3Br and HBr. Based on flame structure measurements and calculations, they suggested that inhibition occurred through reduction of radical generation in the "preignition" part of the flame. In a numerical modeling study, Westbrook [17] argued that HBr has its maximum effect in a temperature range between about 1000 and 1400 K, where the reaction of H atom with HBr competes with its reaction with CH_4 or O_2. In more recent work, Williams and Fleming [16] also describe CF_3Br as reducing H-atom concentrations significantly in the lower temperature regions of the flame (<1200 K); nonetheless, their data do show

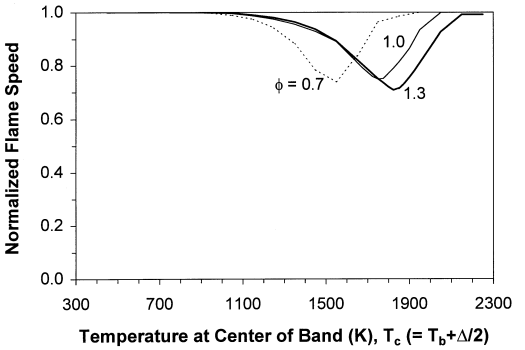

FIG. 4. Effect of damping the rate of the H + O_2 reaction on normalized flame speed for ϕ = 0.7, 1.0, and 1.3.

that the largest absolute reduction in the H-atom volume fraction occurs near 1700 K [16]. Casias and McKinnon [15] also contend that reactions in the low-temperature region are of highest importance for inhibition by CF_3Br, although the conditions of their calculated flames (ethylene/air with 1% CF_3Br) are somewhat different. While our results also show that some of the inhibition effect of HBr and CF_3Br occurs upstream of the locations of the maximum rates for the chain-branching and heat-release reactions, the most sensitive temperature region that we obtain (1600–1900 K) is somewhat higher than argued in these earlier papers.

Figure 4 shows the effect of chain-branching perturbation (Δ = 300 K) on *normalized* flame speed for three equivalence ratios: lean (ϕ = 0.7), stoichiometric (ϕ = 1.0), and rich (ϕ = 1.3). Table 1 lists calculated maximum temperature and flame speed for uninhibited flames at each equivalence ratio. The normalized flame speed is defined as the ratio of the flame speed of a band-inhibited flame to the flame speed of the corresponding uninhibited flame. The temperature of minimum flame speed of the different flames follows the relative position peak of the H-atom volume fraction (see Fig. 5a). The temperature range of maximum influence varies with ϕ, however, because the final temperature of the flame changes with ϕ (see Table 1).

The flame speeds for stoichiometric, rich, and lean flames inhibited by the perfect inhibitor are shown in Fig. 6. The initial volume fraction of perfect inhibitor used for the calculations is the amount needed for a one-third reduction of flame speed (with the inhibiting reactions active throughout the flame) from the uninhibited condition (see Table 1). The value of one-third reduction was selected because it is commonly used in flame inhibition studies; it is a compromise between too little inhibition to show much effect, and too much, for which a real flame would not exist. For band inhibition at the three values of ϕ, the perfect inhibitor shows flame

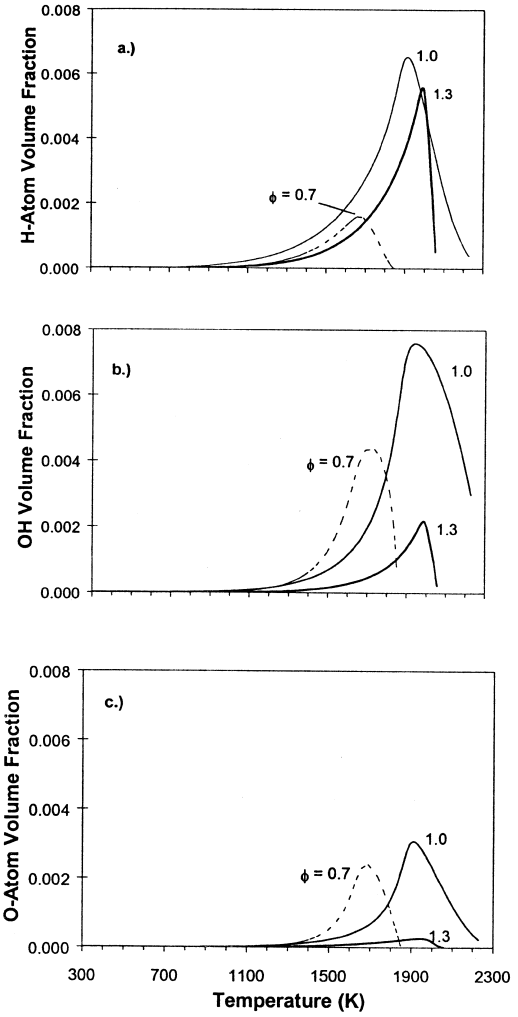

FIG. 5. Calculated volume fraction profiles for H, OH, and O in uninhibited methane/air flames for three stoichiometric ratios. (a) H atom, (b) OH, (c) O atom.

speed reductions qualitatively similar to the results for H + O_2 suppression (as indicated in Table 1): the temperature range for maximum effect is lowest for the lean flame and is higher for stoichiometric and rich flames, which are nearly the same. The ordering follows that of the peak radical volume fractions that are shown in Figs. 5a–c. The calculations generally demonstrate that inhibition in only a small portion of the flame is responsible for most of the inhibitory effect. For example, as shown in Fig. 6, if the inhibiting reactions in the lean flame are turned on between 1500 and 1800 K (T_c = 1650 K), the reduction in flame speed is 65% as much as when the inhibiting reactions occur over the entire flame domain (equivalent results for stoichiometric and rich flames are 72% and 82%).

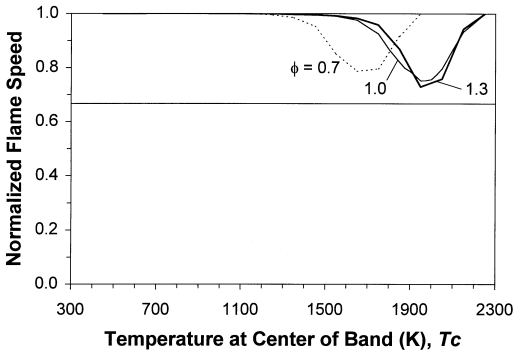

FIG. 6. Effect of the location of perfect inhibition on normalized flame speed for $\phi = 0.7$, 1.0, and 1.3. The horizontal line marks the normalized flame speed when the flames are inhibited throughout the flame.

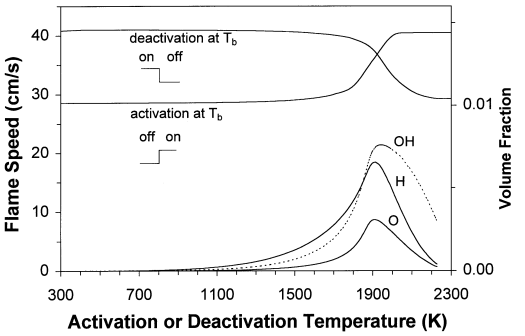

FIG. 7. Variation of flame speed for stepwise inhibitor activation (Fig. 1c) or deactivation (Fig. 1d) for a stoichiometric methane/air mixture. The perfect inhibitor volume fraction is 4.0×10^{-5}. Also shown are calculated volume fraction of OH, H, and O in an uninhibited stoichiometric methane/air flame.

A general result of the calculations presented here for the perfect inhibitor is that perturbation near the region of high radical volume fraction has the strongest effect on flame speed. In other words, removing H atoms from the high-temperature region before they can diffuse upstream has the strongest effect on flame speed because inhibition reactions are faster in regions of high radical volume fraction and high temperature. The results for CF_3Br, however, show that the shift of the partial equilibrium at high temperature for certain reactions can influence the region of maximum influence of the agent.

Potentially effective new fire suppressants may involve an agent that is inert and non-toxic at storage temperature and releases an effective fire suppressant via decomposition or evaporation when added to a fire [26]. For example, the commonly used agent $NaHCO_3$ decomposes at a certain temperature [27] to release the active scavenging species into the gas phase. To simulate such a system, we use a step function (as opposed to the impulse function in the previous section). The shape of the B_i function is illustrated in Fig. 1c. Below the "activation temperature" the inhibition reactions are turned off, and above the activation temperature the inhibition reactions are turned on. For ease of calculation, we use the perfect inhibitor model (with inhibitor volume fraction of 4.0×10^{-5}). The curve labeled "activation" in Fig. 7 shows the flame speed resulting from inhibitor activation at different temperatures between 300 and 2200 K. The flame speed is fairly constant up to about 1700 K, but then starts to increase. The location of the increase coincides with the peak radical concentration. As the activation occurs later in the flame, the inhibitor has less time to scavenge radicals.

Another interesting situation is an active inhibitor that decomposes at a certain temperature and loses its inhibition power. In practice, this might occur due to formation of a condensed-phase species. For example, with $Fe(CO)_5$ inhibition, the active gas-phase species are lost because of condensation to particles at some point in the flame [28]. Since the particle formation appears to be related to the residence time, the deactivation might occur over a range of temperatures. We simulate the stepwise deactivation with a band in which the B_i function (illustrated in Fig. 1d) is a mirror image of the previous example. Above the "deactivation" temperature the inhibition reactions are turned off, and below the deactivation temperature the inhibition reactions are turned on. As in the stepwise activation calculations, the effect of the inhibitor is more or less constant until about 1700 K. The very small reduction in flame speed when the inhibitor is active between 300 and 1700 K reaffirms the importance of the high-temperature reactions. The most important region for the perfect inhibitor is above 1700 K for a strong effect on the flame speed; hence, particle formation for $Fe(CO)_5$ inhibition must be retarded until after the active species have reached the region of about 1700 K.

Conclusion

Premixed flame inhibition has been examined using model inhibitors with reaction rates spatially varied in the flame. The results indicate that for agents which catalytically recombine radicals, the flame speed of a stoichiometric CH_4/air premixed flame is most reduced when the perturbation is near the region of maximum radical volume fraction or the region of maximum rates of the radical scavenging reactions, depending upon the kinetic mechanism of the particular inhibitor. Calculations for CF_3Br-inhibited flames demonstrate a temperature of maximum influence near 1750 K, which is significantly higher than previously suggested. The perturbations

have a negligible effect in the region of the flame temperature below 1200 K.

For flames of varying equivalence ratio, ϕ = 0.7–1.3, perturbation of the $H + O_2 \leftrightarrow OH + O$ reaction rate or addition of the perfect inhibitor have a maximum burning velocity reduction in a temperature region which follows the relative position of the peak H-atom volume fraction. The calculations show that inhibition in a relatively small portion of the flame can cause a significant reduction in flame speed. In some cases, inhibition in a band spanning only 300 K causes nearly as much reduction in flame speed as when the inhibiting reactions are turned on everywhere.

Sudden activation and deactivation of the perfect inhibitor are simulated in a stoichiometric flame. In both cases, the effect of the inhibitor is small when the activation or deactivation temperature is above or below 1700 K, respectively. Hence, new inhibitors that may be developed need not become active until near 1700 K and must not lose their effectiveness until about 2150 K if they are to retain their maximum potential effectiveness.

The results suggest that while the properties of an actual chemical inhibitor which scavenges radicals may cause it to act in a particular region of the flame (perhaps the lower temperature region), the most effective inhibition would result if the agent can act in the regions of high radical volume fraction and flux of the peak chain-branching reaction. It is important to note that these conclusions might be different for other fuels, inhibitors, or flame types.

Acknowledgments

This research was supported by DOD SERDP's Next Generation Fire Suppression Technology Program and by NASA's Office of Biological and Physical Research. The authors thank Dr. D. Burgess for his insightful comments and suggestions.

REFERENCES

1. Fristrom, R. M., and Westenberg, A. A., *Flame Structure,* McGraw-Hill, New York, 1965.
2. Glassman, I., *Combustion,* Academic Press, New York, 1977.
3. Westbrook, C. K., and Dryer, F. L., *Prog. Energy Combust. Sci.* 10:1 (1984).
4. Williams, F. A., *Combustion Theory,* Benjamin/Cummings, Menlo Park, CA, 1985.
5. Levy, A., Droege, J. W., Tighe, J. J., and Foster, J. F., *Proc. Combust. Inst.* 8:524 (1962).
6. Pownall, C., and Simmons, R. F., *Proc. Combust. Inst.* 8:585 (1962).
7. Wilson, W. E., *Proc. Combust. Inst.* 10:47 (1964).
8. Wilson, W. E., O'Donavan, J. T., and Fristrom, R. M., *Proc. Combust. Inst.* 12:929 (1968).
9. Day, M. J., Stamp, D. V., Thompson, K., and Dixon-Lewis, G., *Proc. Combust. Inst.* 13:705 (1970).
10. Fristrom, R. M., and Sawyer, R. F., AGARD Conference on Aircraft Fuels, Lubricants, and Fire Safety, AGARD-CP 84-71, North Atlantic Treaty Organization, Neuilly-sur-seine, France, 1971, 12:2.
11. Biordi, J. C., Lazzara, C. P., and Papp, J. F., *Proc. Combust. Inst.* 14:367 (1972).
12. Dixon-Lewis, G., and Simpson, R. J., *Proc. Combust. Inst.* 16:1111 (1976).
13. Westbrook, C. K., *Combust. Sci. Technol.* 23:191 (1980).
14. Babushok, V., Noto, T., Burgess, D. R., Hamins, A., and Tsang, W., *Combust. Flame* 107:351 (1996).
15. Casias, C. R., and McKinnon, J. T., *Proc. Combust. Inst.* 27:2731 (1998).
16. Williams, B. A., and Fleming, J. W., in *Halon Options Technical Working Conference,* Center for Global Environment Technologies, Albuquerque, NM, 2001, pp. 144–154.
17. Westbrook, C. K., *Combust. Sci. Technol.* 34:201 (1983).
18. Kee, R. J., Grcar, J. F., Smooke, M. D., and Miller, J. A., *A Fortran Computer Program for Modeling Steady Laminar One-Dimensional Premixed Flames,* Sandia report SAND85-8240.
19. Kee, R. J., Rupley, F. M., and Miller, J. A., *CHEMKIN-II: A Fortran Chemical Kinetics Package for the Analysis of Gas Phase Chemical Kinetics,* Sandia report SAND89-8009B.
20. Kee, R. J., Dixon-Lewis, G., Warnatz, J., Coltrin, R. E., and Miller, J. A., *A Fortran Computer Package for the Evaluation of Gas-Phase, Multicomponent Transport Properties,* Sandia report SAND86-8246.
21. Burgess, D. R., *An Interactive, Graphics Postprocessor for Numerical Simulations of Chemical Kinetics,* National Institute of Standards and Technology, 1998, www.nist.gov/cstl/div836/xsenkplot.
22. Linteris, G. T., and Truett, L., *Combust. Flame* 105:15 (1996).
23. Frenklach, M., Wang, H., Yu, C.-L., Goldenberg, M., Bowman, C. T., Hanson, R. K., Davidson, D. F., Chang, E. J., Smith, G. P., Golden, D. M., Gardiner, W. C., and Lissianski, V., *GRI-Mech: An Optimized Detailed Chemical Reaction Mechanism for Methane Combustion,* Gas Research Institute topical report GRI-95/0058, Gas Research Institute, Chicago, IL, 1995, www.me.berkeley.edu/gri_mech.
24. Noto, T., Babushok, V., Burgess Jr., D. R., Hamins, A., Tsang, W., and Miziolek, A., *Proc. Combust. Inst.* 26:1377 (1996).
25. Babushok, V., Tsang, W., Linteris, G. T., and Reinelt, D., *Combust. Flame* 115:551 (1998).
26. Linteris, G. T., and Chelliah, H. K., *Powder-Matrix Systems for Safer Handling and Storage of Suppression Agents,* NISTIR 6766, National Institute of Standards and Technology, Gaithersburg, MD, 2001.
27. Chelliah, H. K., Krauss, R. H., Zhou, H., and Lentati, A. M., paper AJTE99 6121, in *Proceedings of the Fifth ASME/JSME Joint Thermal Engineering Conferences,* ASME, 1999.
28. Rumminger, M. D., and Linteris, G. T., *Combust. Flame* 123:82 (2000).

COMMENTS

Takashi Tsuruda, National Research Institute of Fire and Disaster, Japan. If you change chemical reaction, the flame structure is also affected, like e.g., the temperature distribution. Do you take this change into account in your model?

Author's Reply. Yes. Aside from restricting the region where a sub-set of the chemical reactions can occur, all of the usual equations describing the premixed flame structure are calculated. These include the CHEMKIN/PREMIX equations of mass, species, and energy conservation; hence the temperature field is solved explicitly for the system examined.

•

Pierre Van Tiggelen, University catholique de Louvain, Belgium. Have you tried your method with less efficient inhibitors (for instance CF_3H)? I suspect the efficiency of CF_3Br as an inhibitor is due to the fact that it acts at the right position in the flame (temperature wise) where the branching reaction ($H + O_2 \rightarrow OH + O$) is governing the whole process.

Author's Reply. We appreciate this interesting question from Prof. Van Tiggelen. We have not used the present numerical approach for fluorinated inhibitors such as CF_3H, but have a similar suspicion that the results would be different from those of CF_3Br and the perfect inhibitor. Since CF_3H acts in some ways like a fuel species, the radical pool does not build up until the CF_3H is consumed. Hence, one can surmise that the region of influence of CF_3H would be shifted to a slightly lower temperature region than in the CF_3Br-inhibited flame (as described below). Of course, CF_3H also acts as a thermal diluent. It would be of interest in future work to examine how its effectiveness both as a radical trapping agent and a thermal diluent depend upon the region in the flame where these inhibiting mechanisms are allowed to occur.

•

C. K. Westbrook, LLNL, USA. There are two suggestions for possible improvements to this fine kinetic modeling study. First, use a fuel different from methane (e.g. propane), since methane is somewhat uncharacteristic of "typical" HC fuels. Its flame is already somewhat starved for radicals, so its response to inhibitors may be atypical. Second, include a figure of d[fuel]/dt to test correlations of radical concentrations, temperature windows, etc. with radical reactions with the fuel.

Author's Reply. We thank Dr. Westbrook for the questions (and for his invaluable early work in this area, which inspired the present investigations). We agree that it would be of interest to do the calculations for larger, more reactive hydrocarbons, and hope that we, or others have the opportunity to do this in future work. Examining our numerical results from an uninhibited stoichiometric methane-air flame, we find the point of maximum rate of fuel consumption to be at the location where the temperature is 1662 K. This location is close to, but slightly upstream of, the temperature region of maximum band effectiveness for inhibition by CF_3Br (1750 K), and somewhat further upstream from the point of peak radical mole fraction (1930 K) and of maximum band effectiveness for the perfect inhibitor (1970 K).